Supporting Information

Gupta et al. 10.1073/pnas.1209060109

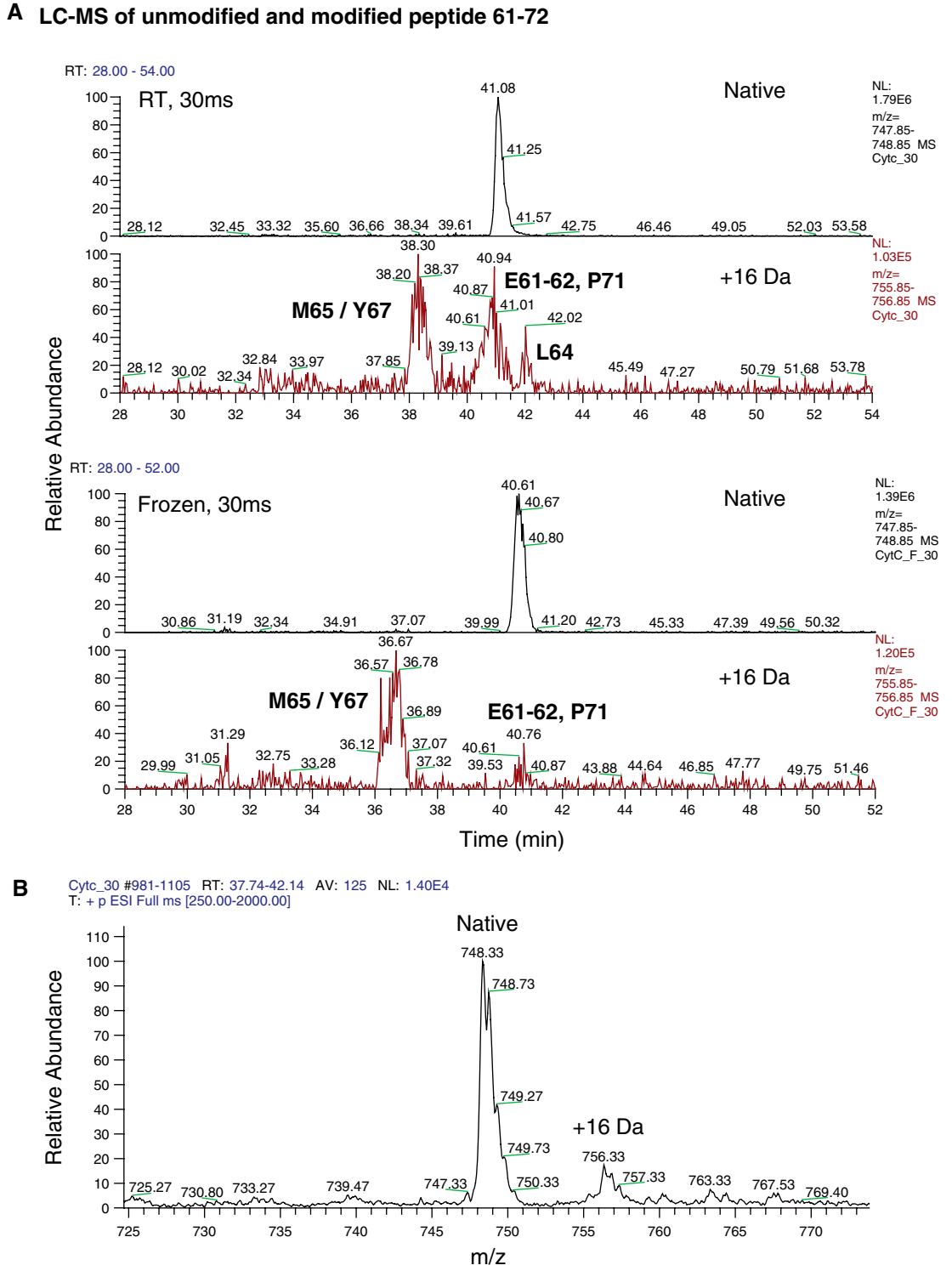

Fig. S1. Example of LC-MS. (*A*) Selected ion chromatogram (SIC) shows the abundance of doubly protonated ($z = 2$) unmodified (748.33 m/z) and modified (+16 Da, 756.33 m/z) peptide 61–72 of 10 μM cyt *c* irradiated for 30 ms at room temperature (RT, 25 °C) and frozen state (−35 °C). Site of modifications are confirmed by MS/MS (Fig. S2). The abundance of modified M65/Y67 are nearly the same at RT and the frozen state, while that for modified E61-62 and P71 are remarkably different. In this example the modified peptide fragments were eluted as a separate peak. The ability to chromatographically isolate the different

species is critical for the analysis. (*B*) The average abundance of unmodified and modified peptide fragment extracted from 37.7–42.1 min. The various fractions of modifications plotted in Figs. S3 and S4*A* are calculated from each of the SICs for all the detected peptides.

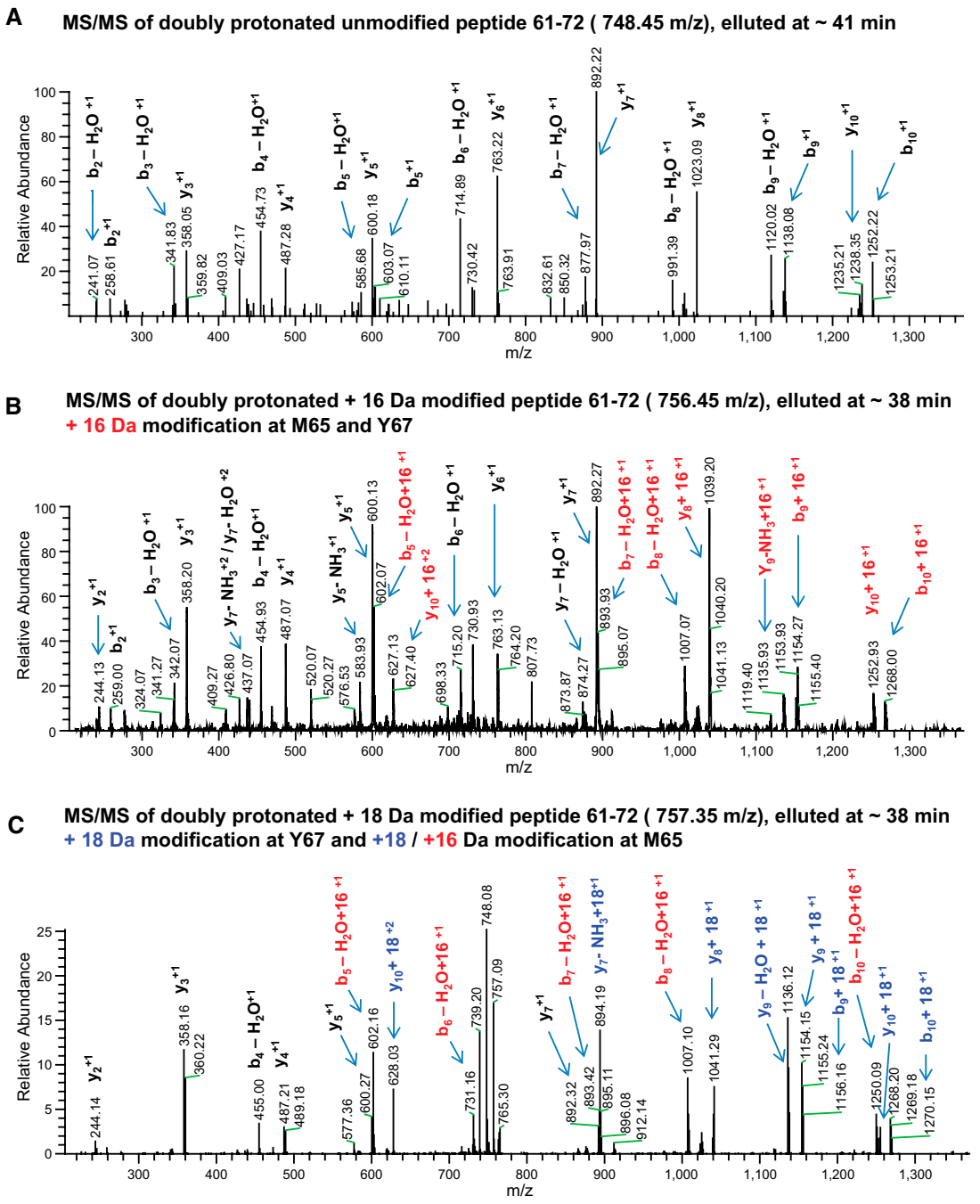

Fig. S2. Identification of site of modifications in ^{16}O- and ^{18}O-labeled peptide 61–72. (*a*) MS/MS spectra of unmodified peptide fragment that eluted at approximately 41 min (Fig. S1) matches with the sequence of peptide 61–72. The MS/MS analysis was carried out with 10 μM cyt *c* in 100% $H_2{}^{16}O$ irradiated for "zero" ms at room temperature (RT, 25 °C). (*B*) MS/MS spectra of modified (+16 Da) peptide fragment that eluted at approximately 38 min (Fig. S1). Presence of unmodified fragment ions b_6-H_2O^{+1} and $y_6{}^{+1}$ together with other modified b and y ions indicate ^{16}O labeling at M65 and Y67 positions. MS/MS analysis was carried out with 10 μM cyt-*c* in 100% $H_2{}^{16}O$ irradiated for 30 ms at room temperature (RT, 25 °C). (*C*) MS/MS spectra of modified (+18 Da) peptide fragment that eluted at approximately 38 min shows ^{18}O labeling at M65 and Y67 positions. MS/MS analysis was carried out with 10 μM cyt *c* in approximately 97% $H_2{}^{18}O$ irradiated for 30 ms at room temperature (RT, 25 °C). The abundance of +16 shifted b ions (b_5-$H_2O + 16^{+1}$ and b_6-$H_2O + 16^{+1}$) indicate the presence of ^{16}O-labeling at M65. Identification of y and b ions was carried out manually with the aid of Protein Prospector v5.10.0 (University of California, San Francisco). MS/MS analysis of other peptides was performed in the similar way.

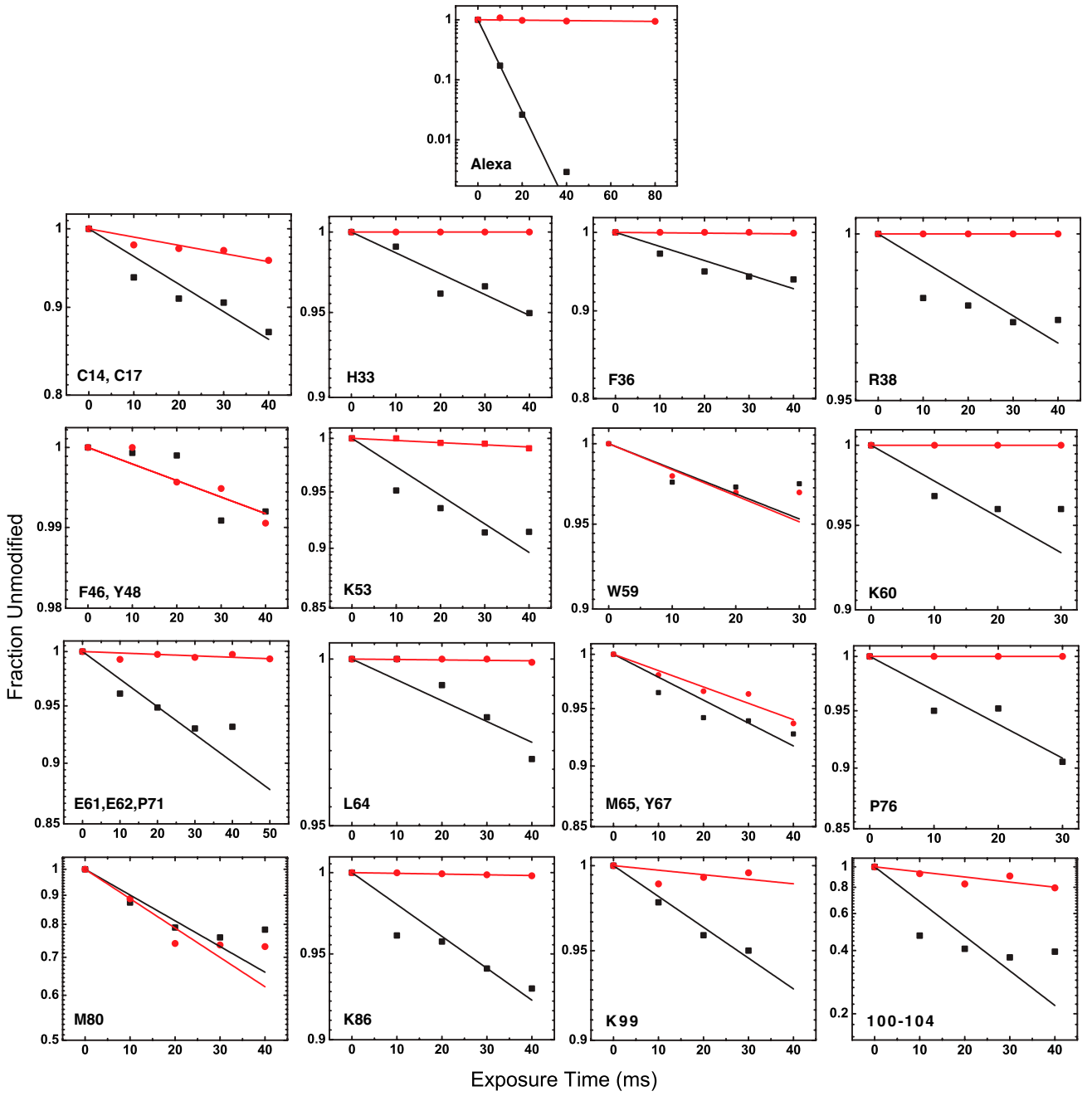

Fig. S3. Comparison of the dose response plots of radiolytic labeling at room temperature (black) and at frozen state (red) for Alexa 488 and the modified side chains of cyt *c*. Alexa solution in 5-μL volume inside each PCR tube is given a single-shot irradiation dose in 0- to 40-ms range. After irradiation the solution is diluted (1:500) prior to fluorescence analysis. A Turner Biosystems TBS-380 fluorometer is used to determine the emission intensity at 516 nm with an excitation wavelength of 496 nm. Upon radiolysis of Alexa 488 in water, its intensity of fluorescence decreases rapidly ($k = 176\ s^{-1}$), while for Alexa 488 irradiated at −35 °C the rate of modification is reduced by more than 200-fold ($k = 0.8\ s^{-1}$). The fraction of unmodified peptide at any exposure is calculated by the unmodified peak area divided by the sum of unmodified and modified peak area. Peak areas are determined from the respective SICs. The peak areas are calculated from the selected ion chromatogram (Fig. S1). A time evolution of SICs is used to calculate fraction unmodified vs. exposure time. The solid line represents the fitting of data to a first-order reaction kinetics [$y = \exp(-k \cdot t)$]. Hydroxyl radical modification rate constant (k, s^{-1}) of the peptide is assigned for the modified residue(s) identified by the MS/MS analysis (Fig. S2). Rate constants are compared between the liquid and frozen states. Plot of T47 is not shown.

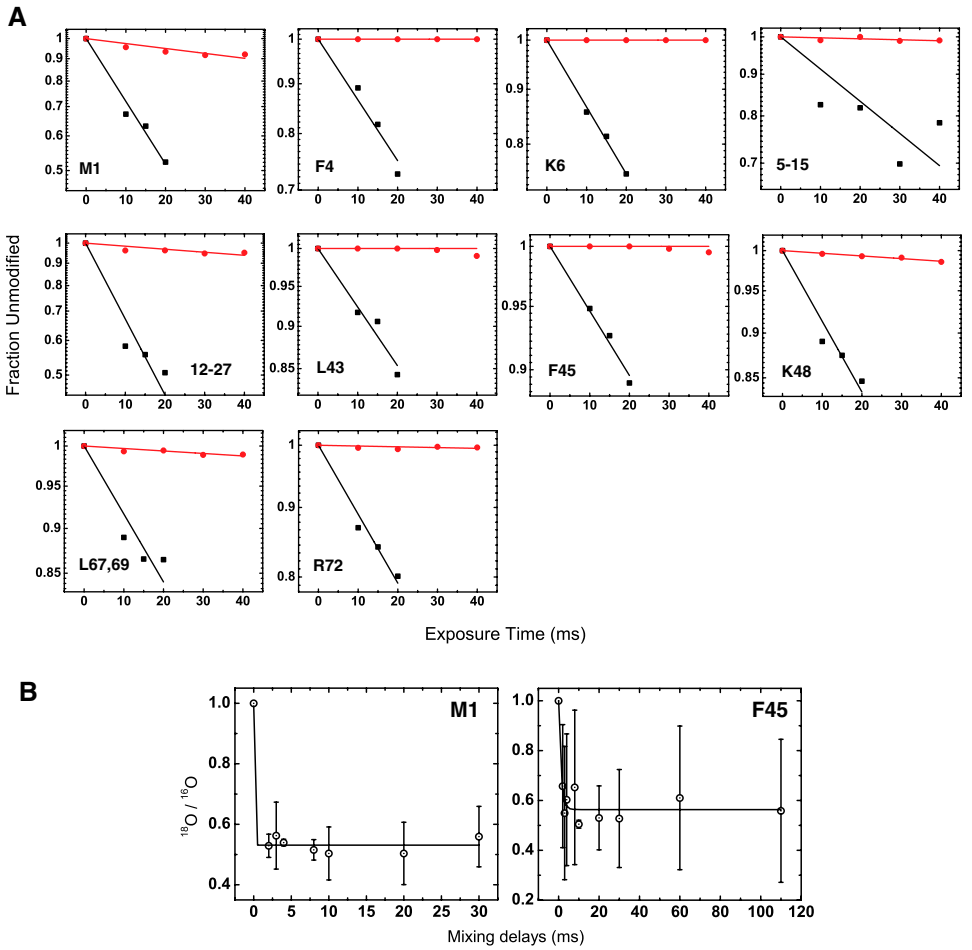

Fig. S4. (*A*) Comparison of the dose response plots of radiolytic labeling at room temperature (black) and at frozen state (red) for the modified side chains of ubiquitin. The fraction of unmodified peptide at any exposure is calculated by the unmodified peak area divided by the sum of unmodified and modified peak area. Peak areas are determined from the respective SICs. The peak areas are calculated from the selected ion chromatogram (similar to Fig. S1). A time evolution of SICs is used to calculate fraction unmodified vs. exposure time. The solid line represents the fitting of data to a first-order reaction kinetics [$y = \exp(-k \cdot t)$]. Hydroxyl radical modification rate constant (k, s^{-1}) of the peptide is assigned for the modified residue(s) identified by the MS/MS analysis. Rate constants are compared between the liquid and frozen states of ubiquitin. (*B*) Time-resolved radiolytic ^{18}O labeling and water exchange in ubiquitin. Progress curves (circles and error bars) for M1 and F45 are fitted to single exponential functions (solid line). Both residues show fast exchanges that are beyond the scope of our current detection limit.

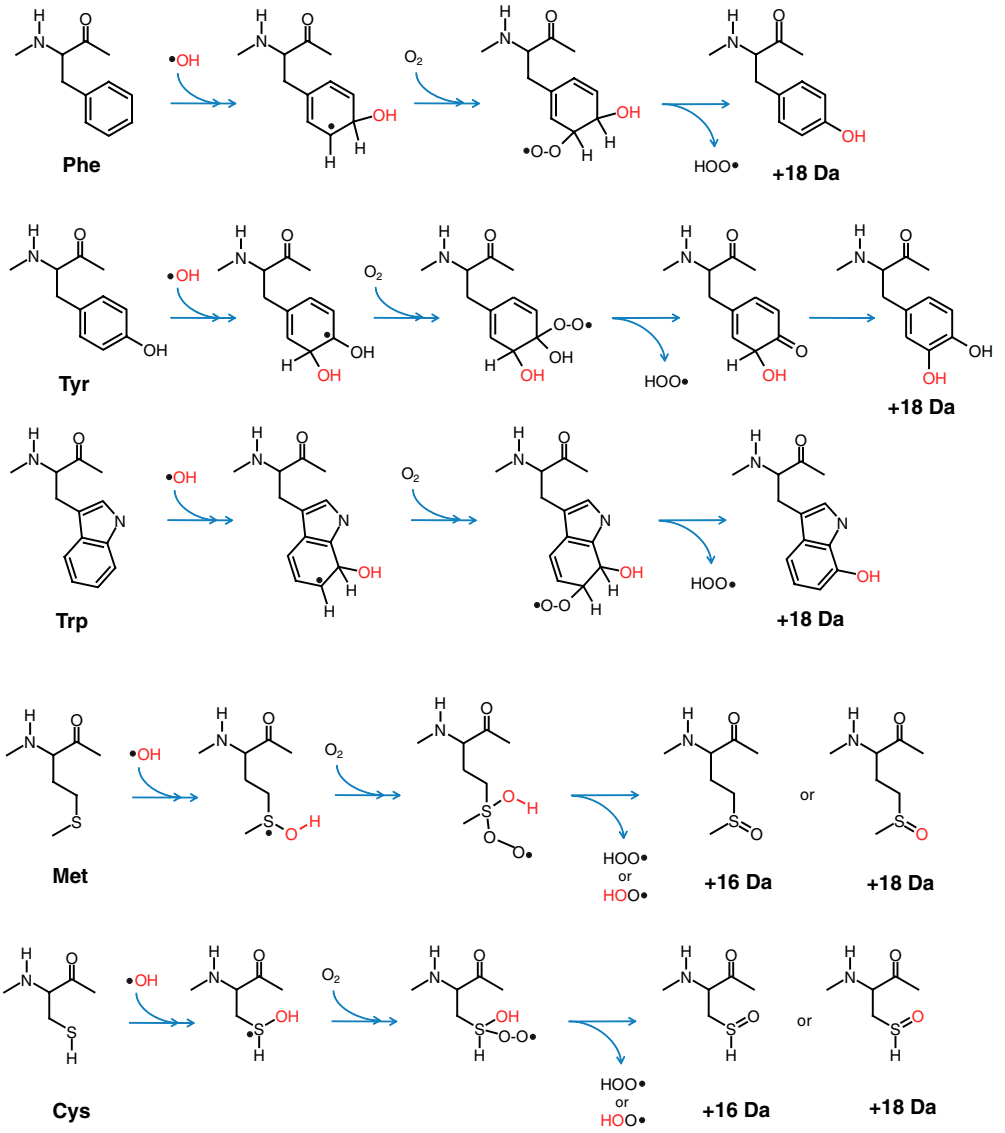

Fig. S5. Reaction schemes for the incorporation of ^{18}O in Phe, Tyr, Trp, Met, and Cys. In the case of addition to π bonds, the direct addition OH• to aromatic rings results in a resonance delocalized radical, which is rearomatized by the loss O_2 addition followed by elimination of hydroperoxyl ion. Following this mechanism, the final product should retain the O-atom from the original OH•. Sulfur-containing side-chain residues form one electron adduct with OH•, and the subsequent addition of O_2 followed by elimination of hydroperoxyl ion generates modified sulfoxides. Following this mechanism the O-atom is derived either from O_2 or OH•. Thus, upon irradiating solutions containing $H_2{}^{18}O$, ^{18}OH• will be generated, which will selectively label these residues and give rise to their corresponding +18 Da modification products. Mass spectrometry analysis in zoom scan mode can provide a quantitative analysis of isotopologues, and MS/MS can identify the location of ^{18}O incorporation.

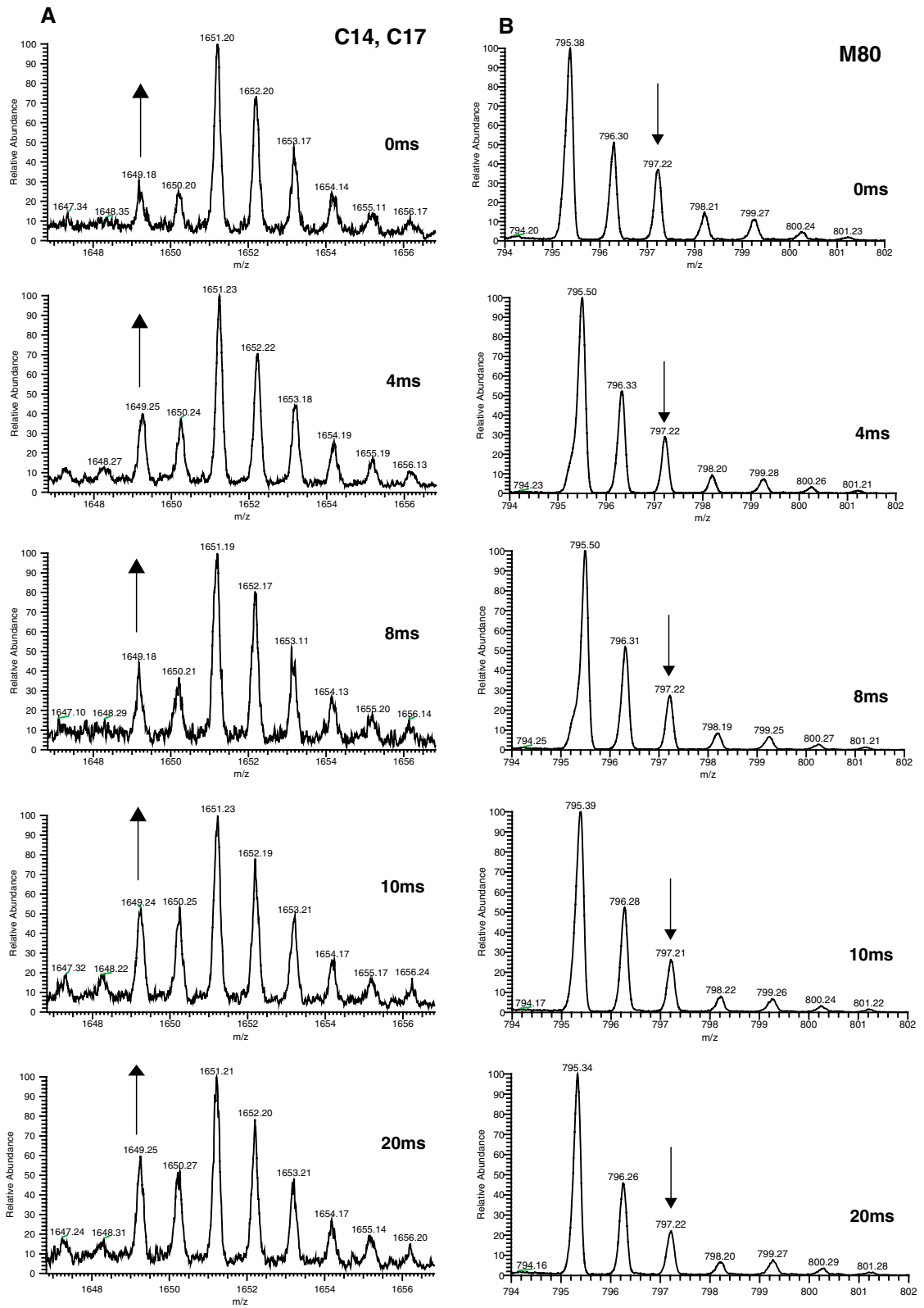

Fig. S6. Zoom scan of peptides after various mixing delays. (*A*) The figure represented the normalized distribution of isotopologues with respect to the third isotopologue peak of peptide 9–22 after various mixing delays. The arrows indicate the increase in the ^{16}O-labeled peptide species with increase in the mixing delays. (*B*) The figure represented the normalized distribution of isotopologues with respect to the first isotopologue peak of peptide 80–86 after various mixing delays. The arrows indicate the decrease in the ^{18}O-labeled peptide species with increase in the mixing delays.

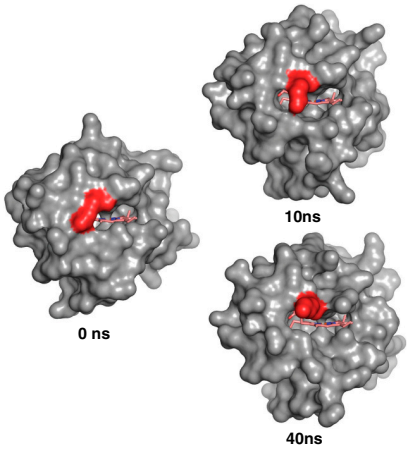

Fig. S7. Molecular dynamics (MD) simulations of cyt *c*. The figure shows surface representation on cyt *c* after 10 and 40 ns. Opening of heme binding pocket during the course of simulation highlighting rotation of K79 (red) is shown. The opening facilitates the navigation of water molecules to and from heme binding pocket. The details of MD follow. Crystal structure of horse heart cyt *c* solved at 1.90 Å resolution was retrieved from the Protein Data Bank (PDB ID code 1HRC) (1). Atomic representation of the protein was prepared using psfgen package of VMD employing CHARMM27 all-atom force field. The energetically relaxed conformation of the solvated cyt *c* was subjected to MD simulations using NAMD (2). The system was gradually heated from 0 to 300 K at the rate of 10 K/ps and equilibrated at 300 K and 1 atm pressure for a total of 1 ns. Langevin dynamics was performed with damping coefficient of 5/ps for controlling fluctuations in temperature, and barostat fluctuations were regulated via standard methods. Atomic representation of the protein was prepared using psfgen package of VMD (3) employing CHARMM27 all-atom force field (4). The heme prosthetic group was represented with iron in oxidized state using force-field parameters from Autenrieth et al. (5). Protein was solvated with approximately 4,800 TIP3P (6) water molecules in a rectangular box ($62 \times 55 \times 62$ Å). Coordinates for the water box were generated using scripts available in MMTSB Tool Set (7). Eight chloride ions were added to neutralize the system. Langevin dynamics was performed with damping coefficient of 5/ps for controlling fluctuations in temperature, and barostat fluctuations were regulated via modified Nosé-Hoover method (8, 9). Two-step energy minimization of the solvated system was performed. In the first step, all the atoms of protein and heme were held fixed while water and counter-ions were relaxed. Force constant of 10 and 5 Kcal/mol per $Å^2$ was applied to harmonically constrain both main-chain and heme atoms, and side-chain atoms, respectively. Minimization was performed for 5,000 steps with nonbonded interactions truncated at 12 Å. In the second step, all restraints were removed and the system was minimized for 10,000 steps. Adjustment in the volume of simulation box was allowed during equilibration stage. Simulations were performed under periodic boundary conditions and particle mesh Ewald (PME) was used to treat long-range electrostatic interactions. For nonbonded interaction switching function was applied with switching distance of 10 Å and cutoff value of 12 Å. Nonbonded interactions were excluded with a value of scaled one-four, implying that all covalently bonded atom pairs were excluded from nonbonded interaction calculation. Also excluded were atom pairs connected to a common third atom. Electrostatic interactions between first and fourth atoms of dihedral angles were scaled by a factor of one. Pairwise nonbonded interactions were searched within distance threshold of 16 Å and the list of nonbonded pairs was updated every 0.04 ps. SHAKE algorithm (10) (with tolerance value of $1.0E^{-8}$) was employed to prevent alteration in interatomic distance between covalently bonded hydrogen and heavy atom pairs. Following equilibration, production simulation was performed for total of 40 ns in isothermal-isochoric ensemble. Temperature was set at 300 K, and volume of the periodic box was fixed to that of equilibrated system. Newtonian equation of motions was integrated every 2 fs, and the snapshots of the dynamic simulation were saved at 2-ps intervals. Structural comparison of the snapshots from the production run with the initial conformation showed that the average backbone heavy atom root-mean-square deviation of snapshots with respect to energy minimized crystal structure was 1.09 ± 0.24 Å. During the simulation, water molecules interact with protein and tend to occupy different sites offering favorable interaction(s). In the crystal structure, the side chain of K79 hydrogen bonds with main-chain of T47 (distance between K79NZ and T47O of 2.7 Å); the observed orientation of K79 rotamer blocking heme access in the crystal structure is likely a consequence of lattice packing, and this rotamer is free to provide water access to the heme in solution (Fig. S7)

1 Bushnell GW, Louie GV, Brayer GD (1990) High-resolution three-dimensional structure of horse heart cytochrome c. *J Mol Biol* 214:585–595.
2 Phillips JC, et al. (2005) Scalable molecular dynamics with NAMD. *J Comput Chem* 26:1781–1802.
3 Humphrey W, Dalke A, Schulten K (1996) VMD: Visual molecular dynamics. *J Mol Graph* 14:33–38.
4 MacKerell AD, et al. (1998) All-atom empirical potential for molecular modeling and dynamics studies of proteins. *J Phys Chem B* 102:3586–3616.
5 Autenrieth F, Tajkhorshid E, Baudry J, Luthey-Schulten Z (2004) Classical force field parameters for the heme prosthetic group of cytochrome c. *J Comput Chem* 25:1613–1622.
6 Jorgensen WL, Chandrasekhar J, Madura JD, Impey RW, Klein ML (1983) Comparison of simple potential functions for simulating liquid water. *J Chem Phys* 79:926–935.
7 Feig M, Karanicolas J, Brooks CL, 3rd. (2004) MMTSB tool set: Enhanced sampling and multiscale modeling methods for applications in structural biology. *J Mol Graph Model* 22:377–395.
8 Feller SE, Zhang Y, Pastor RW, Brooks BR (1995) Constant pressure molecular dynamics simulation: The Langevin piston method. *J Chem Phys* 103:4613–4621.
9 Martyna GJ, Tobias DJ, Klein ML (1994) Constant pressure molecular dynamics algorithms. *J Chem Phys* 101:4177–4189.
10 Ryckaert J-P, Ciccotti G, Berendsen HJC, (1977) Numerical integration of the cartesian equations of motion of a system with constraints: Molecular dynamics of n-alkanes. *J Comput Phys* 23:327–341.

Table S1. Sites of modification and rate constants of hydroxyl radical modifications for cyt-*c*

Sequence number*	Sequence of the trypsin fragments and sites of modification†	Modification rate constant‡, k s^{-1}								
		At room temperature (25 °C)			At −35 °C			At −192 °C		
		SIC peak 1§	SIC peak 2	SIC peak 3	SIC peak 1	SIC peak 2	SIC peak 3	SIC peak 1	SIC peak 2	SIC peak 3
9–22	IFVQK**C**AQ**C**HTVEK	3.7 ± 0.3 C14 (0)¶, C17 (3)	—	—	1.1 ± 0.3 C14, C17	—	—	0.6 ± 0.1 C14, C17	—	—
28–38	TGPNL**H**GL**F**G**R**	1.8 ± 0.1 F36 (50)	0.8 ± 0.1 R38 (51)	1.3 ± 0.1 H33 (35)	nd	nd	nd	nd	nd	nd
40–53	TGQAPG**FTY**TDAN**K**	2.8 ± 0.2 K53 (102)	0.6 ± 0.1 T47 (105)	0.21 ± 0.03 F46 (34), Y48 (14)	0.2 ± 0.02 K53	nd	0.22 ± 0.04 F46, Y48	nd	nd	nd
56–60	GIT**WK**	1.6 ± 0.2 W59 (1)	2.3 ± 0.2 K60 (113)	—	1.7 ± 0.2 W59	nd	—	0.3 ± 0.1 W59	nd	—
61–72	**EETLM**EYLEN**P**K	2.6 ± 0.2 M65 (23) Y67 (0)	2.3 ± 0.2 E61 (81), E62 (134), P71 (0.2)	0.7 ± 0.1 L64 (0)	1.6 ± 0.2 M65 Y67	0.14 ± 0.1 E61-62, P71	—	0.6 ± 0.2 M65 Y67	0.1 ± 0.04 E61-62, P71	—
74–79	Y**I**P**G**TK	3.2 ± 0.3 P76 (94)	—	—	nd	—	—	nd	—	—
80–86	**M**IFAG**I**K	10.5 ± 1 M80 (0)	2.0 ± 0.1 K86 (160)	—	11.9 ± 1 M80	nd	—	1.4 ± 0.2 M80	nd	—
92–99	EDLIAYL**K**	1.9 ± 0.1 K99 (99)	—	—	0.2 ± 0.1 K99	—	—	—	—	—
100–104	KATNE‖	38.0 ± 6.1	—	—	5.6 ± 1.3	—	—	—	—	—

Dash (—) indicates absence of any peak in the SIC. "nd" indicates no detectable modification or rate constant is lower than 0.05 s^{-1}.

*Eighty-five percent sequence coverage was obtained from the LC-ESI-MS analysis of trypsin digest.

†Sequences of tryptic fragments and position of modified residues, which were identified by LC-ESI-MS (Fig. S1) and confirmed by MS/MS (Fig. 2 *A* and *B*).

‡Rate constants were estimated by employing a nonlinear fit of hydroxyl radical modification data to a first-order decay as described in experimental procedures and Fig. S3.

§Modified peptide fragments were eluted as a single peak or multiple peaks in the total ion chromatogram and extracted individually by SIC (Fig. S1). MS/MS analysis shows that a single modification peak either shows modification at only one site (e.g., H33, F36, R38, T47, K53, W59, K60, L64, P76, M80, and K86) or more than one site (e.g., C14/C17, F46/Y48, M65/Y67).

¶Solvent-accessible surface area of modified side chain calculated by MODELLER.

‖Peptide fragment 100–104 showed mixed modification product, which could not be assigned to a particular residue by targeted MS/MS.

Table S2. Sites of modification and rate constants of hydroxyl radical modifications for ubiquitin

Sequence number*	Sequence of the trypsin and pepsin fragments and sites of modification†	Modification rate constant‡, k s^{-1}					
		At room temperature (25 °C)			At −30 °C		
		SIC peak 1§	SIC peak 2	SIC peak 3	SIC peak 1	SIC peak 2	SIC peak 3
1–6	**MQIFVK**	33.3 ± 3.0 M1 (12)¶,	14.3 ± 1.0 F4 (31)	14.2 ± 0.3 K6 (99)	2.6 ± 0.3 M1	nd	nd
5–15	V**KTLT**GK**TI**TL	9.1 ± 1.8 K6 (99), T7 (18), L8 (138), T9 (126), T12 (60), I13 (6)	—	—	0.3 ± 0.05 K6 (99), T7 (18), L8 (138), T9 (126), T12 (60), I13 (6)	—	—
12–27	**TI**TLEVE**P**SDT**I**E**NVK**	40 ± 4.5 T12 (60), I13 (6), P19 (52), E24 (113), N25 (50), V26 (0), K27 (16)	—	—	1.6 ± 0.2 T12, I13, P19, E24, N25, V26, K27	—	—
43–48	**LIF**AG**K**	5.5 ± 0.2 F45 (21)	8.0 ± 0.5 L43 (0), I44 (29)	9.1 ± 0.7 K48 (100)	nd	nd	0.3 ± 0.01 K48 (100)
55–63	TLSDYNIQK	—	—	—	—	—	—
64–72	**ESTLHLVLR**	8.7 ± 0.9 L67 (0), L69 (2)	11.6 ± 0.62 E64 (97), R72 (117)	nd	0.3 ± 0.03 L67 (0), L69 (2)	nd	nd

Dash (—) indicates absence of any peak in the SIC. "nd" indicates no detectable modification or rate constant is lower than 0.05 s^{-1}.

*Eighty-seven percent sequence coverage was obtained from the LC-ESI-MS analysis of tryptic and peptic digests.

†Sequences of tryptic and peptic fragments and position of modified residues, which were identified by LC-ESI-MS and confirmed by MS/MS.

‡Rate constants were estimated by employing a nonlinear fit of hydroxyl radical modification data to a first-order decay as described in experimental procedures and Fig. S4*A*.

§Modified peptide fragments were eluted as a single peak or multiple peaks like that of the cyt-*c*.

¶Solvent-accessible surface area of modified side chain calculated by MODELLER.